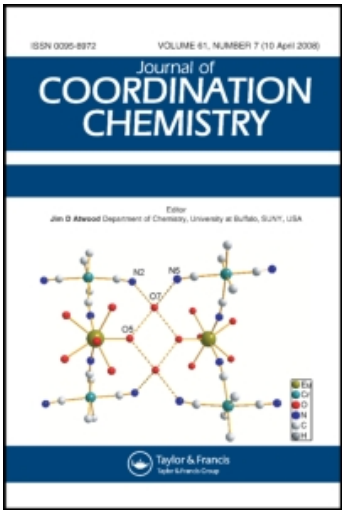

Journal of Coordination Chemistry
Publication details, including instructions for authors and subscription information:
http://www.informaworld.com/smpp/title~content=t713455674

Syntheses, crystal structures, and magnetic properties of five new coordination compounds bearing ferrocenedicarboxylate ligands

Xia Li[a]; Ben-Lai Wu[a]; Wei Liu[b]; Cao-Yuan Niu[a]; Yun-Yin Niu[a]; Hong-Yun Zhang[a]
[a] Department of Chemistry, Zhengzhou University, Zhengzhou, P.R. China [b] Department of Chemistry and Chemical Engineering, Pingdingshan Engineering College, Pingdingshan, P.R. China

To cite this Article Li, Xia , Wu, Ben-Lai , Liu, Wei , Niu, Cao-Yuan , Niu, Yun-Yin and Zhang, Hong-Yun(2009) 'Syntheses, crystal structures, and magnetic properties of five new coordination compounds bearing ferrocenedicarboxylate ligands', Journal of Coordination Chemistry, 62: 19, 3142 — 3156
To link to this Article: DOI: 10.1080/00958970903045280
URL: http://dx.doi.org/10.1080/00958970903045280

Journal of Coordination Chemistry
Vol. 62, No. 19, 10 October 2009, 3142–3156

Syntheses, crystal structures, and magnetic properties of five new coordination compounds bearing ferrocenedicarboxylate ligands

XIA LI†, BEN-LAI WU*†, WEI LIU‡, CAO-YUAN NIU†, YUN-YIN NIU† and HONG-YUN ZHANG*†

†Department of Chemistry, Zhengzhou University, Zhengzhou, 450052, P.R. China
‡Department of Chemistry and Chemical Engineering, Pingdingshan Engineering College, Pingdingshan, 467001, P.R. China

(*Received 11 February 2009; in final form 23 March 2009*)

Five new coordination compounds, $\{[Mn(L)(CH_3OH)_2]\cdot CH_3OH\cdot H_2O\}_n$ (**1**), $\{[Cd(L)(DMF)_2(H_2O)]\cdot H_2O\}_n$ (**2**), $\{[Co(L)(CH_3OH)_4]\cdot CH_3OH\}_2$ (**3**), $\{[Cd(L)(phen)(CH_3OH)]\cdot CH_3OH\}_n$ (**4**), and $\{[Mn(L)(phen)(H_2O)]\cdot CH_3OH\}_n$ (**5**) (L = 5-ferrocene-1,3-benzenedicarboxylic acid, phen = 1,10-phenanthroline) were obtained from different metal salts and L with or without 1,10-phen under mild conditions. Complex **1** is a 1-D ladder-like chain composed of 8-membered rings A and 16-membered rings B, which arrange alternately. Complex **2** is an infinite linear chain, further bridged to form a parallel double chain through different hydrogen-bond interactions. Complex **3** is a discrete dinuclear structure, while **4** is a neutral 1-D infinite zigzag coordination chain. Complex **5** is a 1-D linear chain with phen and ferrocene groups of L as pendants hanging on the different sides of the main chain. Variable temperature magnetic susceptibilities of **1** were measured and weak antiferromagnetic exchange interactions between the neighboring Mn(II) ions were found with $J = -0.95\,cm^{-1}$.

Keywords: Ferrocene-containing dicarboxylate; Coordination compound; Magnetic properties; Mn(II) complex; Cd(II) complex

1. Introduction

Metal-organic frameworks (MOFs) have attracted great interest for their intriguing topological structures and potential application in magnetism, luminescence, gas storage, ion-exchange, optical properties, etc. [1]. In the rational design of such materials, a promising approach is selecting multifunctional bridging ligands. Carboxylate-containing ligands, as an important family of multidentate O-donors, have drawn much attention due to the diversity of connecting modes, high structural stability, and capability as H-bond donor or acceptor. Numerous rigid [2] or flexible [3] carboxylate-containing ligands have been used in constructing MOFs.

Chemists are strongly interested in introducing ferrocene [4] groups into a ligand framework with the objective of generating materials possessing useful electrochemical,

*Corresponding authors. Email: wbl@zzu.edu.cn; wzhy917@zzu.edu.cn

ISSN 0095-8972 print/ISSN 1029-0389 online © 2009 Taylor & Francis
DOI: 10.1080/00958970903045280

magnetic, optical, and nonlinear optical properties [5]. Incorporating carboxyl groups into a ferrocene backbone with multidentate O-donor ligands allows functional metal-organic materials with high structural diversity and stability; numerous ferrocene-containing carboxylate complexes [6–8] have been reported, most derived from ferrocenecarboxylic acid [6] and 1,1′-ferrocenedicarboxylic acid [7]. However, complexes based on ferrocene-containing aromatic dicarboxylate ligands are rarely reported. We are interested in coordination chemistry of a V-shaped ferrocene-containing dicarboxylate ligand, 5-ferrocene-1,3-benzenedicarboxylic acid, and recently reported Co(II) and Zn(II) complexes based on this ligand. Bite angles of the secondary ligands result in substantial structural differences [9]. In this article, we wish to report preparations, crystal structures, electrochemical, thermal, and magnetic properties of five new coordination compounds: $\{[Mn(L)(CH_3OH)_2]\cdot CH_3OH\cdot H_2O\}_n$ (**1**), $\{[Cd(L)(DMF)_2(H_2O)]\cdot H_2O\}_n$ (**2**), $\{[Co(L)(CH_3OH)_4]\cdot CH_3OH\}_2$ (**3**), $\{[Cd(L)(phen)(CH_3OH)]\cdot CH_3OH\}_n$ (**4**), $\{[Mn(L)(phen)(H_2O)]\cdot CH_3OH\}_n$ (**5**) (L = 5-ferrocene-1,3-benzenedicarboxylic acid, phen = 1,10-phenanthroline).

2. Experimental

2.1. *Materials and methods*

5-Ferrocene-1,3-benzenedicarboxylic acid was prepared according to literature method [9]. All other chemicals were obtained from commercial sources and used without purification. IR spectra were recorded on a Bruker VECTOR22 spectrophotometer with KBr pellets from 400–4000 cm^{-1}. Element analyses were performed with a Carlo-Erba 1106 elemental analyzer. Thermal analysis curves were scanned from 30 to 800°C in air on a STA 409 PC thermal analyzer. Differential pulse voltammetry studies were recorded with a CHI650 electrochemical analyzer utilizing the three-electrode configuration of a GC working electrode, a Pt auxiliary electrode, and a saturated calomel electrode as the reference electrode. The measurements were performed in H_2O and DMF ($V_{H2O}:V_{DMF} = 1:4$) containing tetrabutyl ammonium perchlorate (TBAP, 0.1 mol L^{-1}) as the supporting electrolyte. DPV curves were recorded at 20 mV S^{-1} with pulse width of 50 ms and sample width of 20 ms. The potential was scanned from 0 to 1.0 V. Temperature-dependent magnetic measurements were determined on a Quantum Design MPMS-5 magnetometer.

2.2. *Syntheses*

2.2.1. $\{[Mn(L)(CH_3OH)_2]\cdot CH_3OH\cdot H_2O\}_n$ (1). A methanol solution (10 mL) of L (0.035 g, 0.1 mmol) was added dropwise to an aqueous solution (10 mL) of $MnCl_2\cdot 4H_2O$ (0.020 g, 0.1 mmol) and the pH adjusted to about 7 with NaOH aqueous solution. The resulting orange solution was allowed to slowly evaporate at ambient temperature. Two weeks later, orange block single crystals suitable for X-ray single crystal diffraction analysis were obtained in 63% yield based on Mn. Anal. Calcd for $C_{21}H_{26}FeMnO_8$: C, 48.77; H, 5.07. Found: C, 48.52; H, 5.18. IR (KBr, cm^{-1}): 3420 s, 3090 m, 1617 m,

1574 s, 1540 s, 1442 s, 1377 s, 1309 m, 1105 m, 1026 m, 821 m, 785 m, 722 m, 558 m, 493 m, 457 m.

2.2.2. $\{[Cd(L)(DMF)_2(H_2O)]\cdot H_2O\}_n$ (2). A methanol solution (5 mL) of L (0.035 g, 0.1 mmol) was added dropwise to a methanol solution (5 mL) of $Cd(NO_3)_2{\cdot}4H_2O$ (0.030 g, 0.1 mmol), 0.2 mmol NaOH aqueous solution (1 mL) was added, and the resulting precipitate was collected and dissolved in hot DMF. After 1 week, orange block single crystals suitable for X-ray single crystal diffraction analysis were obtained in 38% yield based on Cd. Anal. Calcd for $C_{24}H_{30}CdFeN_2O_8$(%): C, 44.85; H, 4.70; N, 4.36. Found(%): C, 45.23; H, 4.72; N, 4.24. IR (KBr, cm^{-1}): 3426 s, 3106 m, 2642 m, 1605 s, 1561 s, 1442 s, 1372 s, 1106 m, 1029 m, 826 m, 734 m, 495 m, 453 m.

2.2.3. $\{[Co(L)(CH_3OH)_4]\cdot CH_3OH\}_2$ (3). Complex **3** was prepared using a method similar to that for **1** except that $MnCl_2{\cdot}4H_2O$ was replaced by $Co(NO_3)_2{\cdot}6H_2O$. Red needles suitable for X-ray single crystal diffraction analysis were obtained in 49% yield based on Co. Anal. Calcd for $C_{23}H_{28}CoFeO_9$(%): C, 49.05; H, 5.01. Found(%): C, 49.23; H, 4.82. IR (KBr, cm^{-1}): 3404 s, 3093 m, 1618 m, 1562 s, 1442 s, 1379 s, 1106 m, 1029 m, 1001 m, 913 m, 818 m, 780 m, 722 m, 492 m, 451 m.

2.2.4. $\{[Cd(L)(phen)(CH_3OH)]\cdot CH_3OH\}_n$ (4). A methanol solution (10 mL) of phen (0.020 g, 0.1 mmol) was added dropwise to a methanol solution (5 mL) of $Cd(NO_3)_2{\cdot}4H_2O$ (0.030 g, 0.1 mmol), and then a methanol solution (10 mL) of L (0.035 g, 0.1 mmol) was added. With triethylamine slowly diffusing into the mixture for a month, orange block single crystals suitable for X-ray single crystal diffraction analysis were obtained in 51% yield based on Cd. Anal. Calcd for $C_{32}H_{28}CdFeN_2O_6$(%): C, 54.53; H, 4.00; N, 3.97. Found(%): C, 54.23; H, 4.12; N, 4.04. IR (KBr, cm^{-1}): 3417 s, 3087 m, 1554 s, 1428 m, 1368 s, 1102 m, 1027 m, 852 m, 781 m, 730 m, 493 m, 459 m.

2.2.5. $\{[Mn(L)(phen)(H_2O)]\cdot CH_3OH\}_n$ (5). A solution of L (0.035 g, 0.1 mmol) and NaOH (0.008 g, 0.2 mmol) in methanol (15 mL) was carefully layered on an aqueous solution (10 mL) of $MnCl_2{\cdot}4H_2O$ (0.020 g, 0.1 mmol) and phen (0.020 g, 0.1 mmol) in a straight glass tube. About 2 weeks later, orange needles suitable for X-ray analysis were obtained in 56% yield based on Mn. Anal. Calcd for $C_{31}H_{26}FeMnN_2O_6$(%): C, 58.79; H, 4.14; N, 4.42. Found(%): C, 58.68; H, 4.16; N, 4.29. IR (KBr, cm^{-1}): 3424 s, 3095 m, 1614 m, 1560 s, 1516 m, 1445 s, 1392 s, 1105 m, 1037 m, 853 m, 783 m, 730 m, 494 m, 461 m.

2.3. *X-ray structural determination*

Crystallographic data for the compounds were collected at 291(2) K on a Bruker SMART APEX-II CCD diffractometer equipped with a graphite crystal and incident beam monochromator using Mo-Kα radiation ($\lambda = 0.71073$ Å). Absorption corrections were applied using SADABS. The structures were solved with direct methods and refined with full-matrix least-squares techniques on F^2 using SHELXTL [10]. All nonhydrogen atoms were refined anisotropically. Hydrogens were assigned with

common isotropic displacement factors and included in the final refinement by using geometrical restraints. Crystal data are summarized in detail in table 1. Selected bond lengths and angles are listed in table 2.

3. Results and discussion

3.1. *Structure description*

Complex **1** crystallizes in a space group $P2_1/c$. As shown in figure 1, each Mn(II) is coordinated to six oxygens with two oxygens (O1, O2) from one chelating bidentate carboxylate of one L (Mn1–O1 2.223(3), Mn1–O2, 2.356(3) Å), two oxygens (O3, O6) separately from two bridging bidentate carboxylate groups of two other L (Mn1–O3, 2.092(3), Mn1–O6, 2.123(3) Å), and two oxygens (O4, O5) from two methanol molecules (Mn1–O5, 2.195(3), Mn1–O4 2.196(4) Å), giving a slightly distorted octahedral geometry. Atoms O1, O2, O3, and O6 form the equatorial plane with the Mn deviating from the mean plane by 0.0163 Å, and O3 and O5 occupying axial positions. A visible twisting is observed between the cyclopentadienyl ring (Cp) and the linked phenyl ring, with the dihedral angle between them being 33.3°.

Carboxylate groups in each ligand adopt different coordination modes, one chelating bidentate while the other is bridging bidentate. Similar coordination modes have been found for 1,3-benzenedicarboxylate [11]. Each L is connected by three Mn ions, and three Mn ions are bridged by three L to form two rings: 8-membered rings A and 16-membered rings B (figure 1). These rings are arranged alternately resulting in a 1D ladder-like structure, and the F_c groups hang on both sides of the double-strand chain. Distances between adjacent Mn ions in the intrachain are 4.390 and 7.132 Å, respectively.

These adjacent zigzag chains are further connected through O–H···O hydrogen-bond interactions (O–H···O = 2.648–2.869 Å, ⟨O–H···O = 74.7–165°) between solvated waters and coordinated oxygens of carboxylates, and between coordinated methanols and solvated water (table 3), giving a 2D structural motif in the *ab* plane as illustrated in figure 2.

The structure of **2** is a 1-D framework, crystallizing in a monoclinic space group $P2_1/c$. As shown in figure 3, each Cd(II) is distorted octahedral with three oxygens from two different ligands (Cd1–O1, 2.194(2), Cd1–O4, 2.362(2), Cd1–O3, 2.405(3) Å), two oxygens from two coordinated DMF's (Cd1–O7, 2.299(3), Cd1–O5, 2.323(3) Å), and one oxygen from water (Cd1–O6, 2.298(3) Å). The phenyl ring and the Cp ring are almost coplanar with mean deviation from the plane of 0.0279 Å. The two carboxylate groups have 13.9° and 5.1° dihedral angles with the plane of the linked corresponding phenyl ring.

Adjacent Cd(II) ions are linked by monodentate and bis-monodentate carboxylates of L into an infinite linear chain with the F_c groups hanging on the same side. Adjacent linear chains are further bridged to form parallel double chains through different O–H···O (O···O = 2.706–2.843 Å, ⟨O–H···O = 131–167°) hydrogen-bond interactions (table 3), originating from coordinated water hydrogens to uncoordinated oxygens of the carboxylates and lattice water oxygens, or from uncoordinated water hydrogens to coordinated oxygens of carboxylates (figure 4).

Table 1. Crystal data and structure refinement for **1**–**5**.

Complex	**1**	**2**	**3**	**4**	**5**
Formula	$C_{21}H_{26}FeMnO_8$	$C_{24}H_{30}CdFeN_2O_8$	$C_{23}H_{28}CoFeO_9$	$C_{32}H_{28}CdFeN_2O_6$	$C_{31}H_{26}FeMnN_2O_6$
F/w	517.21	642.75	563.23	704.81	633.33
Crystal system	Monoclinic	Monoclinic	Orthorhombic	Monoclinic	Triclinic
Space group	*P21/c*	*P21/c*	*Cmca*	*C2/c*	$P\bar{1}$
Unit cell dimensions (Å, °)					
a	7.745(2)	15.830(3)	17.192(2)	27.802(2)	9.773(2)
b	10.135(3)	10.210(2)	13.2506(18)	10.6163(9)	10.050(2)
c	28.280(8)	17.247(3)	21.311(3)	19.1589(16)	14.307(3)
α	90	90	90	90	94.62(3)
β	95.933(4)	112.33(3)	90	98.3180(10)	102.66(3)
γ	90	90	90	90	93.05(3)
V (Å^3)	2208.0(11)	2578.3(9)	4854.8(11)	5595.3(8)	1362.9(5)
Z	4	4	8	8	2
D_{Calcd} (gcm^{-3})	1.556	1.656	1.541	1.673	1.543
F(000)	1068	1304	2328	2848	650
θ Range (°)	2.48–26.00	2.37–25.50	2.37–25.50	2.27–28.34	2.31–25.50
Index range (°)	$-9 \le h < = 9$, $-12 \le k \le 12$, $-34 \le l \le 34$	$-19 \le h \le 19$, $-12 \le k \le 12$, $-20 \le l \le 20$	$-20 \le h \le 20$, $-16 \le k \le 16$, $-25 \le l \le 25$	$-37 \le h \le 36$, $-13 \le k \le 14$, $-25 \le l \le 25$	$-11 \le h \le 11$, $-12 \le k \le 12$, $-17 \le l \le 16$
Reflections collected/ unique (*R*(int))	14,522/4347 [*R*(int) = 0.0662]	20,479/4765 [*R*(int) = 0.0440]	17,444/2337 [*R*(int) = 0.0304]	21,396/6933 [*R*(int) = 0.0321]	10,193/5040 [*R*(int) = 0.0325]
Goodness-of-fit on F^2	1.042	1.036	1.082	1.032	1.023
R_1, wR_2 ($I > 2\sigma(I)$)	0.0541, 0.1300	0.0343, 0.0803	0.0352, 0.1216	0.0326, 0.0667	0.0400, 0.0936
R_1, wR_2 (all data)	0.0766, 0.1424	0.0487, 0.0868	0.0425, 0.1319	0.0514, 0.0750	0.0604, 0.1054
Largest difference in peak and hole (e Å^{-3})	0.808, −0.653	1.145, −0.929	0.562, −0.406	0.508, −0.600	0.384, −0.328

Table 2. Selected bond distances (Å) and angles (°) for **1**–**5**.

1					
Mn1–O3$^{\#1}$	2.092(3)	Mn1–O6$^{\#2}$	2.123(3)	Mn1–O5	2.195(3)
Mn1–O4	2.196(4)	Mn1–O1	2.223(3)	Mn1–O2	2.356(3)
O3$^{\#1}$–Mn1–O6$^{\#2}$	113.04(11)	O3$^{\#1}$–Mn1–O5	88.19(13)	O6$^{\#2}$–Mn1–O5	89.15(13)
O3$^{\#1}$–Mn1–O4	91.53(14)	O6$^{\#2}$–Mn1–O4	94.80(13)	O5–Mn1–O4	175.82(13)
O3$^{\#1}$–Mn1–O1	99.93(11)	O6$^{\#2}$–Mn1–O1	147.02(10)	O5–Mn1–O1	92.44(13)
O4–Mn1–O1	83.50(12)	O3$^{\#1}$–Mn1–O2	157.05(11)	O6$^{\#2}$–Mn1–O2	89.88(10)
O5–Mn1–O2	91.15(12)	O4–Mn1–O2	87.48(13)	O1–Mn1–O2	57.17(9)
2					
Cd1–O1	2.194(2)	Cd1–O7	2.299(3)	Cd1–O6	2.298(3)
Cd1–O5	2.323(3)	Cd1–O4$^{\#1}$	2.362(2)	Cd1–O3$^{\#1}$	2.405(3)
O1–Cd1–O7	101.78(11)	O1–Cd1–O6	130.78(10)	O7–Cd1–O6	86.69(11)
O1–Cd1–O5	86.71(13)	O7–Cd1–O5	170.79(13)	O6–Cd1–O5	85.02(13)
O1–Cd1–O4$^{\#1}$	89.42(9)	O7–Cd1–O4$^{\#1}$	87.39(10)	O6–Cd1–O4$^{\#1}$	139.71(9)
O5–Cd1–O4$^{\#1}$	96.35(11)	O1–Cd1–O3$^{\#1}$	142.05(9)	O7–Cd1–O3$^{\#1}$	88.53(10)
O6–Cd1–O3$^{\#1}$	85.74(9)	O5–Cd1–O3$^{\#1}$	86.86(12)	O4$^{\#1}$–Cd1–O3$^{\#1}$	54.28(8)
3					
Co1–O2	2.0752(7)	Co1–O2$^{\#1}$	2.0752(7)	Co1–O4$^{\#1}$	2.0893(8)
Co1–O4	2.0893(8)	Co1–O3$^{\#1}$	2.1081(8)	Co1–O3	2.1081(8)
O2–Co1–O2$^{\#1}$	89.00(4)	O2–Co1–O4$^{\#1}$	92.03(3)	O2$^{\#1}$–Co1–O4$^{\#1}$	92.75(3)
O2–Co1–O4	92.75(3)	O2$^{\#1}$–Co1–O4	92.03(3)	O4$^{\#1}$–Co1–O4	173.30(5)
O2–Co1–O3$^{\#1}$	175.94(3)	O2$^{\#1}$–Co1–O3$^{\#1}$	88.58(3)	O4$^{\#1}$–Co1–O3$^{\#1}$	84.84(3)
O4–Co1–O3$^{\#1}$	90.59(3)	O2–Co1–O3	88.58(3)	O2$^{\#1}$–Co1–O3	175.94(3)
O4$^{\#1}$–Co1–O3	90.59(3)	O4–Co1–O3	84.84(3)	O3$^{\#1}$–Co1–O3	94.02(4)
4					
Cd1–N2	2.322(2)	Cd1–O2	2.3355(18)	Cd1–N1	2.364(2)
Cd1–O5	2.382(2)	Cd1–O1	2.4601(19)	Cd1–O4$^{\#1}$	2.1996(18)
O2–Cd1–N1	130.40(8)	N2–Cd1–O2	91.90(8)	N2–Cd1–N1	71.12(8)
O4$^{\#1}$–Cd1–O2	118.43(8)	O4$^{\#1}$–Cd1–N1	90.96(8)	O4$^{\#1}$–Cd1–N2	149.18(7)
O4$^{\#1}$–Cd1–O5	92.69(8)	O2–Cd1–O5	78.70(7)	O4$^{\#1}$–Cd1–O1	94.46(7)
N2–Cd1–O5	87.83(9)	N1–Cd1–O5	142.97(8)	N2–Cd1–O1	108.97(8)
O2–Cd1–O1	53.95(6)	N1–Cd1–O1	87.17(7)	O5–Cd1–O1	129.16(7)
5					
Mn1–O5	2.167(2)	Mn1–O2	2.220(2)	Mn1–N2	2.299(3)
Mn1–N1	2.300(3)	Mn1–O1	2.432(2)	Mn1–O4$^{\#1}$	2.508(2)
Mn1–O3$^{\#1}$	2.185(2)	O3–Mn1$^{\#2}$	2.185(2)	O4–Mn1$^{\#2}$	2.508(2)
O5–Mn1–O3$^{\#1}$	91.55(9)	O5–Mn1–O2	105.37(10)	O3$^{\#1}$–Mn1–O2	84.25(8)
O5–Mn1–N2	164.30(9)	O3$^{\#1}$–Mn1–N2	94.59(9)	O2–Mn1–N2	89.64(9)
O5–Mn1–N1	93.37(9)	O3$^{\#1}$–Mn1–N1	137.66(9)	O2–Mn1–N1	134.05(8)
N2–Mn1–N1	72.43(9)	O5–Mn1–O1	84.49(9)	O3$^{\#1}$–Mn1–O1	136.77(8)
O2–Mn1–O1	55.93(8)	N2–Mn1–O1	100.65(9)	N1–Mn1–O1	85.57(9)
O5–Mn1–O4$^{\#1}$	84.02(9)	O3$^{\#1}$–Mn1–O4$^{\#1}$	55.05(8)	O2–Mn1–O4$^{\#1}$	138.79(8)
N2–Mn1–O4$^{\#1}$	87.67(9)	N1–Mn1–O4$^{\#1}$	83.71(8)	O1–Mn1–O4$^{\#1}$	163.77(7)

Symmetry transformations used to generate equivalent atoms: for **1** $^{(\#1)}$ $-x, -y+1, -z$, $^{(\#2)}$ $x, y+1, z$; for **2** $^{(\#1)}$ $x, y+1, z$; for **3** $^{(\#1)}$ $x, -y, -z+1$; for **4** $^{(\#1)}$ $x, -y+2, z+1/2$; for **5** $^{(\#1)}$ $x, y+1, z$, $^{(\#2)}$ $x, y-1, z$.

Complex **3** crystallizes in the space group *Cmca* and exhibits a discrete dinuclear structure as shown in figure 5. The Co(II) is six-coordinate by two oxygens (O2) from carboxyl groups of two different L and four oxygens (O3 and O4) from methanol. The Co$-$O$_{COO^-}$ distances (2.077 Å) are slightly shorter than those of the Co–O$_{CH_3OH}$ (2.088–2.109 Å). The bond angle of N7$-$Co$-$N7A is 180.0°. Therefore, the local environment around Co(II) can be described as a slightly compressed octahedron. The phenyl ring and the Cp are almost coplanar with mean deviation from the plane being 0.0087 Å. The two carboxylate groups both have 11.4° dihedral angles with the plane of the linked corresponding phenyl rings.

In **3**, each L serves as a bisconnector through two carboxyls, and two ligands bridge two Co(II)'s through carboxylate bridges producing a dinuclear metal ring.

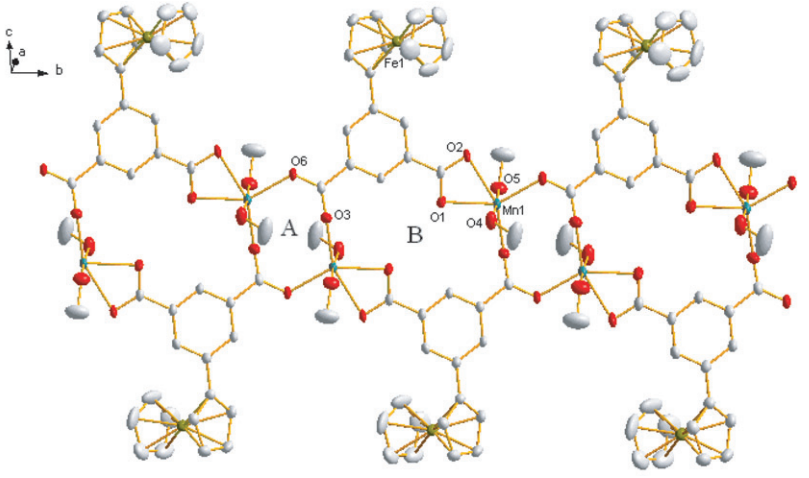

Figure 1. ORTEP drawing with heteroatom labeling scheme of the 1-D ladder chain structure of $\{[Mn(L)(CH_3OH)_2]\cdot CH_3OH\cdot H_2O\}_n$ (**1**) with rings A and B (H atoms and uncoordinated solvent molecules omitted for clarity).

Table 3. Hydrogen bonding distances (Å) and angle (°) data for **1**, **2**, **4,** and **5**.

D–H···A	d(D–H)	d(D···A)	∠(D–H···A)	Symmetry codes
1				
O(4)–H(4A)···O(7)	0.73(7)	2.648(5)	165(8)	$-x, -y+1, -z$
O(8)–H(8A)···O(2)	0.874	2.840	87.3	$x-1, y, z$
O(8)–H(8B)···O(6)	0.863	2.869	74.7	$x-1,1+y, z$
O(5)–H(5A)···O(8)	0.852(10)	2.734(6)	151(6)	
O(7)–H(7A)···O(1)	0.86(7)	2.712(5)	165(7)	
2				
O(6)–H(6B)···O(2)	0.90(6)	2.706(4)	167(6)	$-x, -y, -z$
O(6)–H(6A)···O(8)	0.73(6)	2.843(5)	162(7)	$x, y+1, z$
O(8)–H(8A)···O(3)	0.82(6)	2.745(4)	131(6)	
4				
O(5)–H(5)···O(3)	0.852(10)	2.822(3)	153(4)	$-x, y, -z+1/2$
O(6)–H(6)···O(1)	0.858(10)	2.764(3)	169(5)	
5				
O(5)–H(5B)···O(1)	0.75(4)	2.714(3)	175(5)	$-x-1, -y+1, -z$
O(6)–H(6A)···O(4)	0.84	2.679(4)	154.4	$-x-1, -y+1, -z$
O(5)–H(5A)···O(6)	0.75(4)	2.680(4)	174(5)	

The distance of two Co(II) ions in the metal ring is 7.963 Å. Two ferrocene groups lie above and below on opposite directions of the metal ring.

Single-crystal X-ray diffraction analyses reveal that **4** is a neutral 1-D infinite zigzag coordination chain and crystallizes in the monoclinic *C2/c* space group. Each Cd(II) is six-coordinate by two nitrogens from phen (Cd1–N1 = 2.364(2), Cd1–N2 = 2.322(2) Å), three oxygens from carboxyls of two different L (Cd–O = 2.1997(17) – 2.4601(19) Å), and one oxygen from methanol (Cd1–O5 = 2.382(2) Å), forming a distorted octahedron as shown in figure 6. The phenyl ring and the two carboxylates are almost coplanar with mean deviation from the plane being 0.0497 Å. A visible twisting

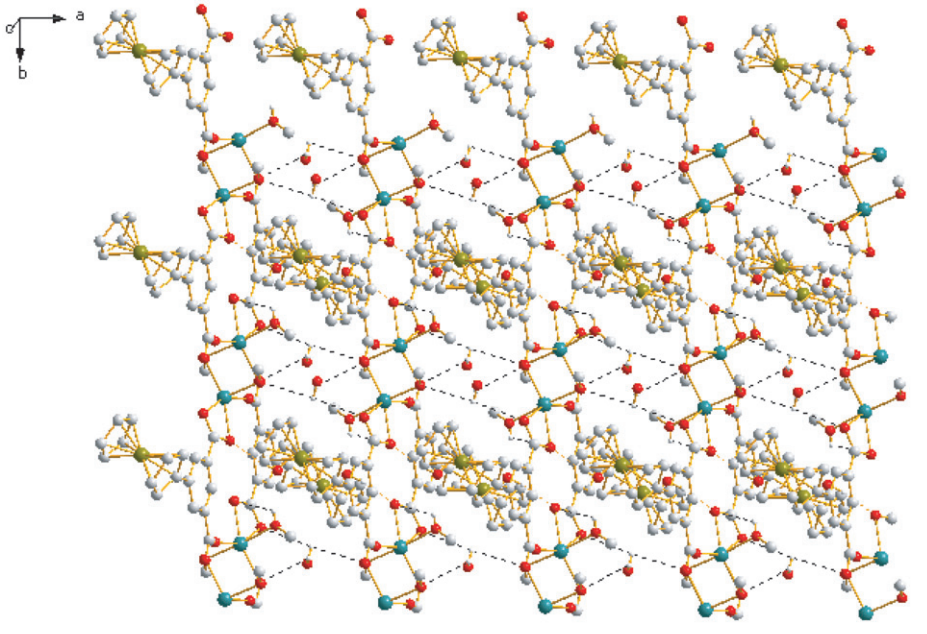

Figure 2. View of 2-D supramolecular network in **1** forming through hydrogen bonds. The hydrogen bonding interactions between the chains are indicated as dotted lines (...).

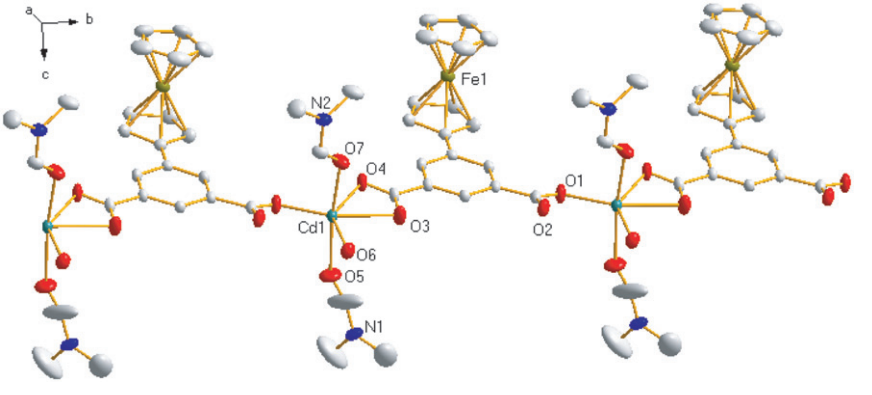

Figure 3. ORTEP drawing with heteroatom labeling scheme of the 1-D linear chain structure of $\{[Cd(L)(DMF)_2(H_2O)] \cdot H_2O\}_n$ (**2**) (H atoms and uncoordinated solvent molecules omitted for clarity).

is observed between the Cp ring and its attached phenyl ring, with the dihedral angle between them being 29.2°.

Each L serving as a bisconnector through its two carboxylates bridges two Cd(II)'s in an infinite 1-D zigzag chain. There are two different coordination modes of the two carboxylates, monodentate, and bidentate chelate. Two adjacent Cd(II) ions separated by L are at 10.226 Å. Adjacent zigzag chains are further bridged to form parallel double chains through O–H···O (O–H···O = 2.822(2) Å, ⟨O–H···O = 153°) hydrogen-bond interactions (table 3), originating from coordinated methanol hydrogens in one coordination chain to the uncoordinated oxygen of carboxylate in the adjacent chain (figure 7).

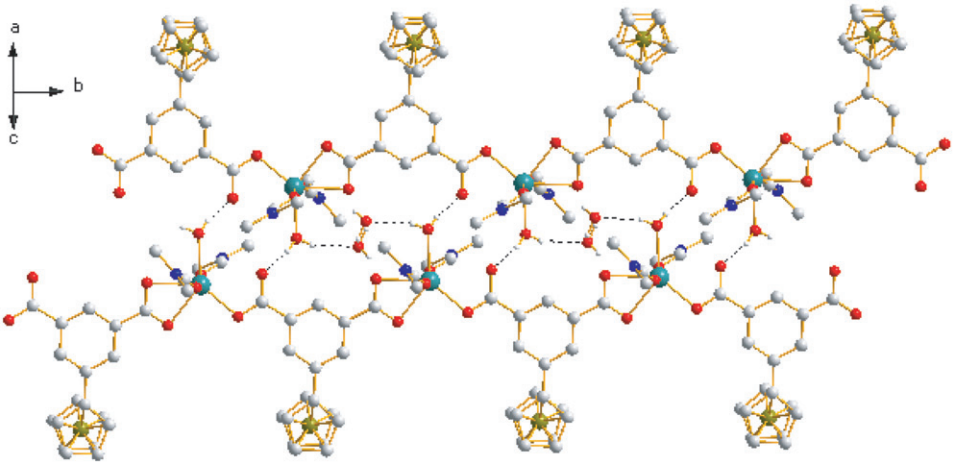

Figure 4. The double linear chains bridged by hydrogen bonding in **2**. The hydrogen bonding interactions between the chains are indicated as dotted lines (...).

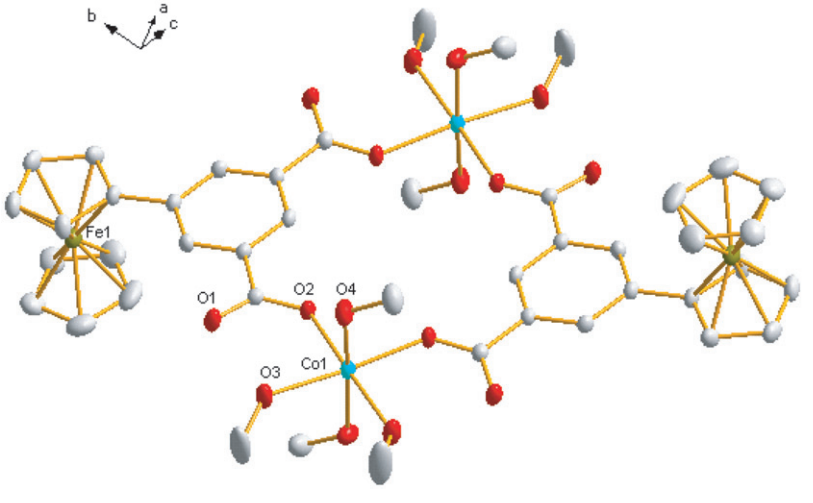

Figure 5. ORTEP drawing with heteroatom labeling scheme of the dinuclear structure of $\{[Co(L)(CH_3OH)_4]\cdot CH_3OH\}_n$ (**3**) (H atoms and uncoordinated solvent molecules omitted for clarity).

Double chains are further extended to a layer network through aromatic ring π–π stacking interactions of 1,10-phen (figure 8), and the closest distance between adjacent aromatic rings is 3.307 Å.

Crystal structure analysis by X-ray diffraction demonstrates that **5** crystallizes in a space group $P\bar{1}$. As shown in figure 9, each Mn(II) is in a distorted octahedral geometry ligated by two nitrogens from 1,10-phen, three oxygens from two different carboxylates of L and one oxygen from water. O1, O2, O3, and N1 form the equatorial plane (deviation of Mn(II) from the mean plane is about 0.2332 Å), and O5 and N2 occupy axial positions (O5–Mn–N2 164.30(9)°). The Mn–O distances range from 2.167(2) to 2.432(2) Å, while the Mn–N distances are 2.299(3) and 2.300(3) Å, respectively.

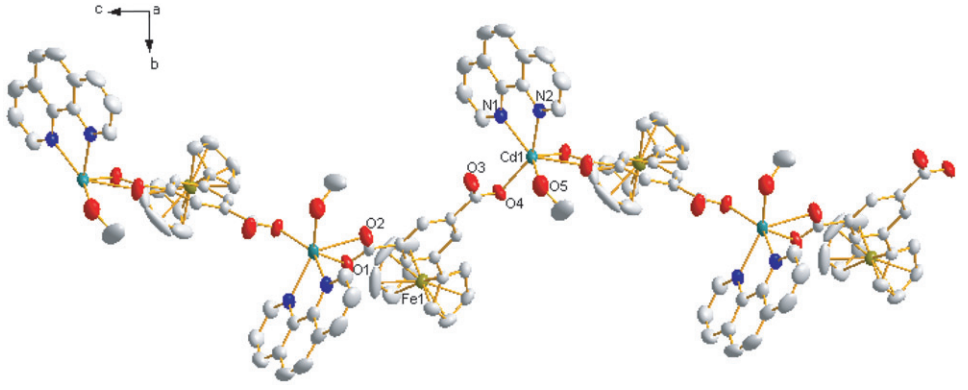

Figure 6. ORTEP drawing with heteroatom labeling scheme of the dinuclear structure of $\{[Cd(L)(phen)(CH_3OH)]\cdot CH_3OH\}_n$ (**4**) (H atoms and uncoordinated solvent molecules omitted for clarity).

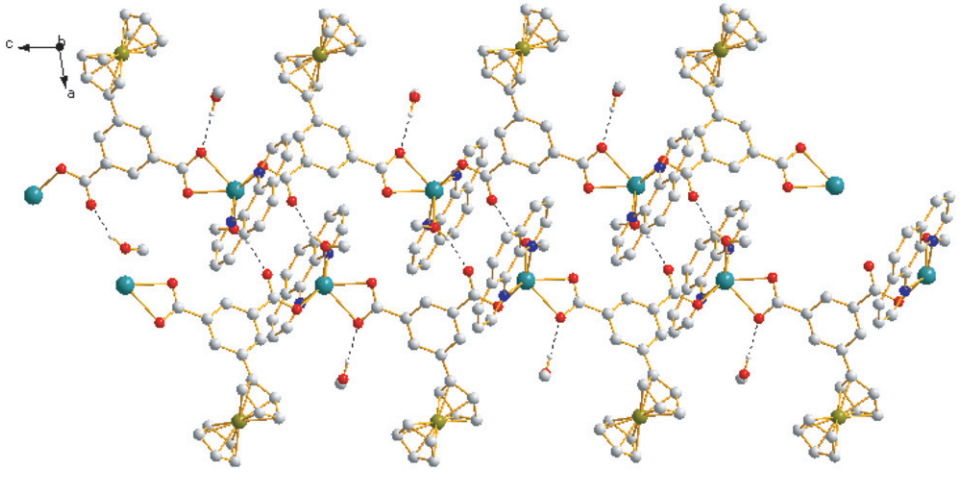

Figure 7. The double linear chains bridged by hydrogen bonding in **4**. The hydrogen bonding interactions between the chains are indicated as dotted lines (...).

In **5**, two carboxylates of L are monodentate and bidentate chelate and each L is a μ_2-bridge linking two Mn(II)'s to give a 1-D linear chain. The distance of two adjacent Mn(II)'s separated by L is 10.050 Å. The ferrocene and 1,10-phen hang parallel on each side of the main chain. The separations between adjacent Mn(II) ions, Fe(II) ions and 1,10-phen rings are all 10.050 Å. Adjacent linear chains are further bridged to form parallel double chains through different O–H···O (O–H···O = 2.679–2.714 Å, ⟨O–H···O = 154–175°) hydrogen-bond interactions (table 3), originating from coordinated water hydrogens and lattice CH_3OH hydrogens, respectively, to uncoordinated oxygen of carboxylate, or from coordinated water hydrogens to lattice CH_3OH oxygens (figure 10). Moreover, double chains are further extended to a layer network through aromatic π–π stacking interactions of the phen (figure 11); the closest distance between adjacent aromatic rings is 3.39 Å.

In **1**–**5**, some coordination sites of the metal are occupied by subsidiary ligand and solvent molecules, limiting the structural dimensionality. In **1**–**3**, each metal center is

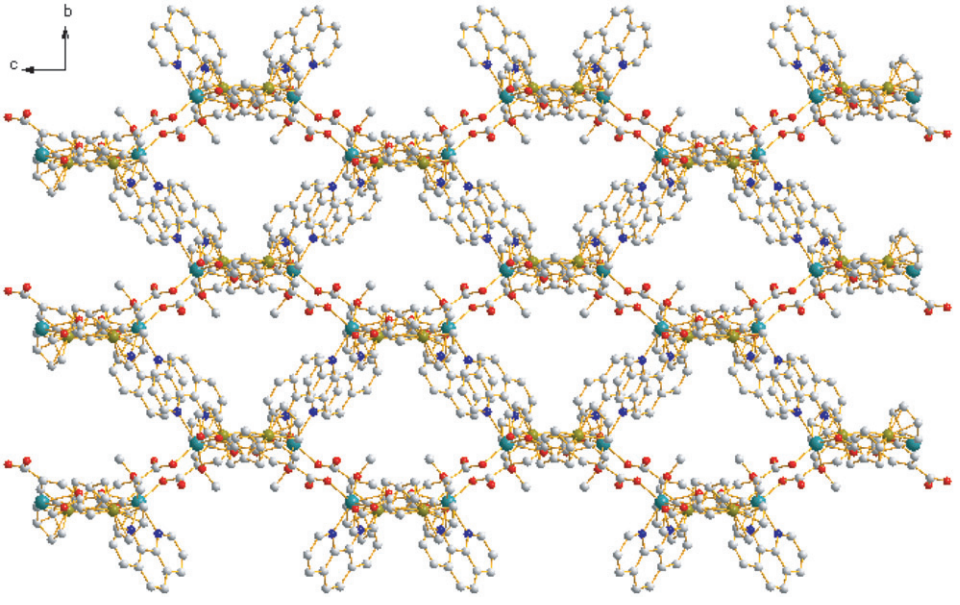

Figure 8. 2-D network of **4** showing the π–π stacking interactions between phen.

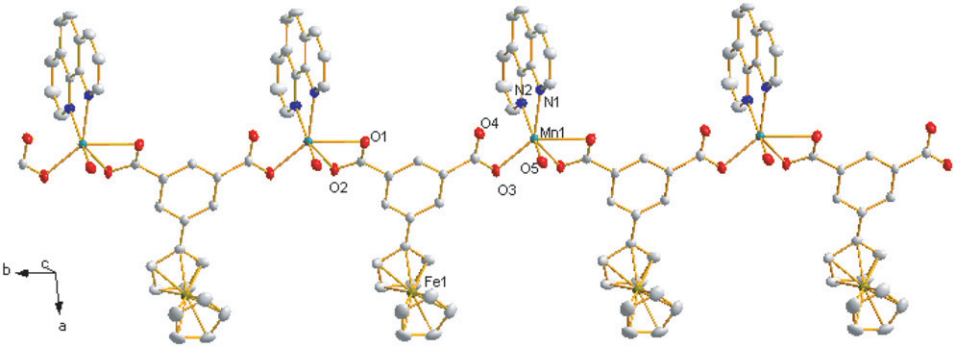

Figure 9. ORTEP drawing with heteroatom labeling scheme of the structure of $\{[Mn(L)(phen)(H_2O)]\cdot CH_3OH\}_n$ (**5**) (H atoms and uncoordinated solvent molecules omitted for clarity).

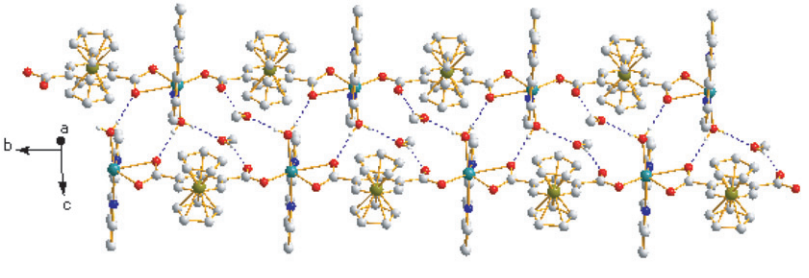

Figure 10. The double linear chains bridged by the hydrogen bonding in **5**. The hydrogen bonding interactions between the chains are indicated as dotted lines (...).

distorted octahedral with different coordination sites posited by solvent resulting in structural diversity. In **4** and **5**, phen does not change the dimensionality of the complexes, but the packing style directed by π–π stacking interactions. The ultimate structures for **4** and **5** come from the different solvents.

3.2. *IR spectroscopy*

Complexes **1**–**5** show similar IR spectra. The absence of absorption bands at 1731–1651 cm^{-1} where the –COOH is expected indicates complete deprotonation of L upon coordination to metal. For **1**, bands at 3090 and 493 cm^{-1} (3106 and 495 cm^{-1} for **2**, 3093 and 492 cm^{-1} for **3**, 3087 and 493 cm^{-1} for **4**, 3095 and 494 cm^{-1} for **5**) are attributed to υ(C–H) and υ(Fe–Cp) vibration of the ferrocenyl group [12]. Strong absorptions at 1574 and 1377 cm^{-1} (1561 and 1372 cm^{-1} for **2**, 1562 and 1379 cm^{-1} for **3**, 1554 and 1368 cm^{-1} for **4**, 1560 and 1392 cm^{-1} for **5**) are due to the asymmetric $\upsilon_{as}(COO^{-})$ and symmetric $\nu_{as}(COO^{-})$ stretching vibrations. The broad bands at around 3420 cm^{-1} are from hydroxyl. IR data are in good agreement with X-ray analyses.

3.3. *Thermogravimetric analysis*

Thermogravimetric analyses of **1**, **4**, and **5** were carried out at a heating rate of 10°C min^{-1} under air.

For **1**, the first weight loss of 17.54% occurred from 86 to 371°C, corresponding to all crystallization and coordinated solvent (Calcd 22.04%). The deviation may be due to easy loss of lattice solvent molecules at ambient temperature. The second weight loss of 51.13% from 371 to 441°C suggests destruction of the framework by oxidation of the organic component (Calcd 56.67%). The residue of 31.33% can be attributed to MnO and Fe_2O_3 (Calcd 29.20%). For **4**, the first weight loss of 4.54% occurred from 86 to 371°C, corresponding to removal of the solvent methanol (Calcd 4.86%). On further

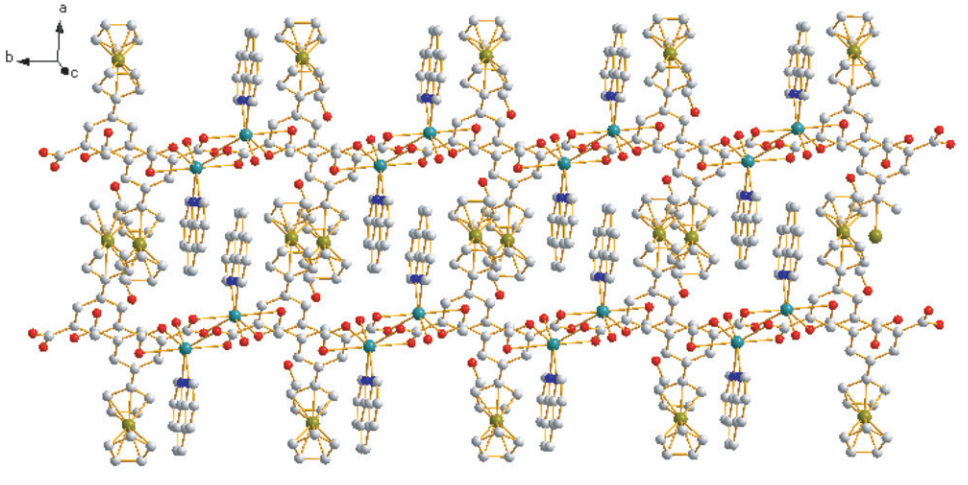

Figure 11. 2-D network of **5** showing the π–π stacking interactions between phen.

heating, loss of coordinated methanol and simultaneous structural decomposition starts. The residue of 31.85% can be attributed to the formation of CdO and Fe_2O_3 (Calcd 29.51%). The structure of **5** remains thermally stable up to 127°C. Then a gradual weight loss of 9.30% to 307°C was observed, corresponding to release of solvated methanol and coordinated water (Calcd 7.58%). On further heating, **5** decomposed rapidly. Total loss of all organic moieties occurred in a series of weight loss steps between 307 and 490°C. The final remaining mass of 25.20% is consistent with a remnant solid of MnO and Fe_2O_3 (Calcd 23.84%).

3.4. *Redox properties*

Electrochemical behavior of **1**–**3** and L were studied by differential pulse voltammetry at a glassy carbon working electrode in mixed solution of H_2O and DMF. Both L and the complexes show a single peak corresponding to the single-electron F_c/F_c^+ couple with the half-wave potential being 416, 430, 418, and 424 mV for L and **1**–**3**, respectively. The electrochemical results show coordinated metal ions do not affect the potential of the F_c/F_c^+ couple in **1**–**3**. Moreover, the half-wave potential of L shifts lower in H_2O and DMF compared with DMF (half-wave potential is 560 mV in DMF [9]).

3.5. *Magnetic properties*

The temperature (T) dependencies of the magnetic susceptibility (χ_M) of **1** were measured from 2 to300 K under fixed fields of 1 kOe and the magnetic susceptibility χ_M and μ_{eff} *versus* T plots are shown in figure 12. The experimental μ_{eff} value at room temperature is 6.05 μ_B, which is close to the expected value (5.92 μ_B) for an isolated spin $S = 5/2$ of Mn(II). Upon cooling from room temperature, μ_{eff} values decrease smoothly until 50 K and sharply at lower temperatures reaching values of 2.62 μ_B at 2.5 K. As shown in the χ_M^{-1} *versus* T plot, all data follow the Curie–Weiss law closely with $C = 4.42$ cm^{3}mol^{-1}K and $\theta = -5.27$ K. Decrease of μ_{eff} upon cooling and the

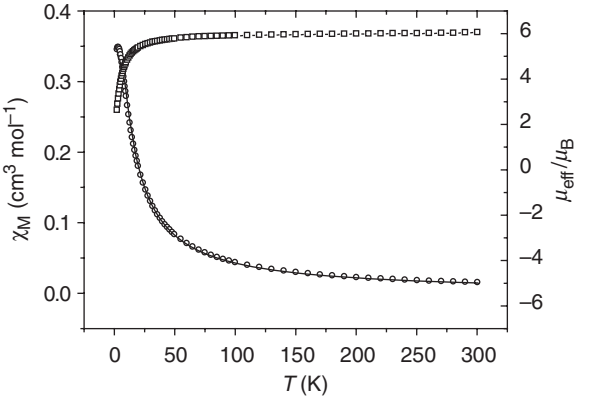

Figure 12. χ_M (○) and μ_{eff} (□) *vs.* T plot with the theoretical fit (—) for **1**.

negative value of θ indicate weak antiferromagnetic interactions between adjacent Mn(II) centers.

Considering the short Mn–Mn separation of 4.390 Å in the 8-membered ring A and the rather long Mn–Mn separation of 7.132 Å in the 16-membered ring B, we simplify the magnetic interactions in **1** between Mn(II) centers as a dinuclear system and fitted through the equation for dimers [13]. The experimental data fit well with parameters $g = 2.02$, $J = -0.95\,\mathrm{cm}^{-1}$, and $R = 1.8 \times 10^{-6}$ ($R = \sum[(\chi_M)_{obsd}] - [(\chi_M)_{cacld}]^2 / \sum[(\chi_M)_{obsd}]^2$. The solid lines in figure 12 represent the best fit of the experimental data.

4. Conclusion

In summary, five new coordination complexes have been constructed by self-assembly of 5-ferrocene-1,3-benzenedicarboxylic acid and different metal salts under mild conditions. Three coordination modes of L have been found in **1**–**5**. Although **1**, **2**, **4**, and **5** are all 1-D chains, their packing interaction are different, and the hydrogen bond and π–π stacking interaction play very important roles in the construction of supramolecular architectures. The magnetic susceptibility study of **1** demonstrates the presence of antiferromagnetic interaction between Mn(II) ions.

Supplementary material

Crystallographic data for the structural analysis have been deposited with the Cambridge Crystallographic Data Center, 671852 for **1**, 710928 for **2**, 710929 for **3**, 663359 for **4**, and 663360 for **5**. Copies of these information may be obtained free of charge at http://www.ccdc.cam.ac.uk/conts/retrieving.html or from the Cambridge Crystallographic Data Centre, 12 Union Road, Cambridge CB2 1EZ, UK [Fax: (+44) 1223-336-033; E-mail: deposit@ccdc.cam.ac.uk].

Acknowledgements

We gratefully acknowledge financial support from the National Natural Science Foundation of China (20771094, 20671083) and the Science and Technology Key Task of Henan Province (0524270061). We also thank Prof. Song Gao and Dr Xiuteng Wang for the magnetic measurement.

References

[1] (a) O.M. Yaghi, H. Li, C. Davis, D. Richardson, T.L. Groy. *Acc. Chem. Res.*, **31**, 474 (1998); (b) M. Eddaoudi, D.B. Moler, H. Li, B. Chen, T.M. Reineke, M. O'Keeffe, O.M. Yaghi. *Acc. Chem. Res.*, **34**, 319 (2001); (c) C.N.R. Rao, S. Natarajan, R. Vaidhyanathan. *Angew. Chem. Int. Ed.*, **43**, 1466 (2004); (d) C. Jainak. *Dalton Trans.*, 2781 (2003).

[2] (a) W.G. Lu, C.Y. Su, T.B. Lu, L. Jiang, J.M. Chen. *J. Am. Chem. Soc.*, **128**, 34 (2006); (b) P.G. Plieger, D.S. Ehler, B.L. Duran, T.P. Taylor, K.D. John, T.S. Keizer, T.M. McCleskey, A.K. Burrell, J.W. Kampf, T. Haase, P.G. Rasmussen, J. Karr. *Inorg. Chem.*, **44**, 5761 (2005); (c) R. Cao, D.F. Sun, Y.C. Liang, M.C. Hong, K. Tatsumi, Q. Shi. *Inorg. Chem.*, **41**, 2087 (2002); (d) Y. Yan, C.D. Wu, X. He, Y.Q. Sun, C.Z. Lu. *Cryst. Growth Des.*, **5**, 821 (2005); (e) B. Zhao, P. Cheng, X.Y. Chen, C. Cheng, W. Shi, D.Z. Liao, S.P. Yan, Z.H. Jiang. *J. Am. Chem. Soc.*, **126**, 3012 (2004); (f) X. Lin, A.J. Blake, C. Wilson, X.Z. Sun, N.R. Champness, M.W. George, P. Hubberstey, R. Mokaya, M. Schroder. *J. Am. Chem. Soc.*, **128**, 10745 (2006).

[3] (a) D.X. Xue, W.X. Zhang, X.M. Chen. *J. Mol. Struct.*, **877**, 36 (2008); (b) S.N. Wang, J.F. Bai, Y.Z. Li, Y. Pan, M. Scheer, X.Z. You. *Cryst. Eng. Comm*, **9**, 1084 (2007); (c) X.J. Zhang, Y.H. Xing, Z. Sun, J. Han, Y.H. Zhang, M.F. Ge, S.Y. Niu. *Cryst. Growth Des.*, **7**, 2041 (2007); (d) Z. Wang, H.H. Zhang, Y.P. Chen, C.C. Huang, R.Q. Sun, Y.N. Cao, X.H. Yu. *J. Solid State Chem.*, **179**, 1536 (2006); (e) H.F. Zhu, J. Fan, T.A. Okamura, Z.H. Zhang, G.X. Liu, K.B. Yu, W.Y. Sun, N. Ueyama. *Inorg. Chem.*, **45**, 3941 (2006); (f) H.F. Zhu, Z.H. Zhang, W.Y. Sun, T. Okamura, N. Ueyama. *Cryst. Growth Des.*, **5**, 177 (2005).

[4] T.J. Kealy, P.L. Pauson. *Nature*, **168**, 1039 (1951).

[5] (a) R.D.A. Hudson. *J. Organomet. Chem.*, **47**, 637 (2001); (b) C.J. Fang, C.Y. Duan, D. Guo, C. He, Q.J. Meng, Z.M. Wang, C.H. Yan. *Chem. Commun.*, 2540 (2001); (c) P.D. Beer, D.K. Smith. *Prog. Inorg. Chem.*, **46**, 1 (1997); (d) Z.H. Wang, K.C. Chen, H. Tian. *Chem. Lett.*, **5**, 423 (1999); (e) B. Bildstein, M. Schweiger, H. Angleitner, H. Kopacka, K. Wurst, K.H. Ongania, M. Fontani, P. Zanello. *Organometallics*, **18**, 4286 (1999); (f) G. Li, Y.L. Song, H.W. Hou, L.K. Li, Y.T. Fan, Y. Zhu, X.R. Meng, L.W. Mi. *Inorg. Chem.*, **42**, 913 (2003).

[6] (a) M.R. Churchill, Y.J. Li, D. Nalewajek, P.M. Schaber, J. Dorfman. *Inorg. Chem.*, **24**, 2684 (1985); (b) S.K.C. Kumara, S. Nagabrahmanandachari, K. Raghuraman. *J. Organomet. Chem.*, **587**, 132 (1999); (c) V. Chandrasekhar, S. Nagendran, S. Bansal, A.W. Cordes, A. Vij. *Organometallics*, **21**, 3297 (2002); (d) V. Chandrasekhar, S. Nagendran, S. Bansal, M.A. Kozee, D.R. Powell. *Angew. Chem. Int. Ed.*, **39**, 1833 (2000); (e) H.W. Hou, L.K. Li, G. Li, Y.T. Fan, Y. Zhu. *Inorg. Chem.*, **42**, 3501 (2003); (f) S.M. Lee, K.K. Cheung, W.T. Wong. *J. Organomet. Chem.*, **506**, 77 (1996); (g) A.L. Abuhijleh, C. Woods. *J. Chem. Soc., Dalton Trans.*, 1249 (1992).

[7] (a) G.L. Zheng, J.F. Ma, Z.M. Su, L.K. Yan, J. Yang, Y.Y. Li, J.F. Liu. *Angew. Chem. Int. Ed. Engl.*, **43**, 2409 (2004); (b) X.R. Meng, H.W. Hou, G. Li, B.X. Ye, T.Z. Ge, Y.T. Fan, Y. Zhu, H. Sakiyama. *J. Organomet. Chem.*, **689**, 1218 (2004); (c) D. Guo, H. Mo, C.Y. Duan, F. Lu, Q.J. Meng. *J. Chem. Soc., Dalton Trans.*, 2593 (2002); (d) S.D. Christie, S. Subramanian, L.K. Thompson, M.J. Zaworotko. *J. Chem. Soc., Chem. Commun.*, 2563 (1994); (e) X.R. Meng, G. Li, H.W. Hou, H.Y. Han, Y.T. Fan, Y. Zhu, C.X. Du. *J. Organomet. Chem.*, **679**, 153 (2003); (f) Y.Y. Yang, W.T. Wong. *Chem. Commun.*, 2716 (2002); (g) D. Guo, B.G. Zhang, C.Y. Duan, X. Cao, Q.J. Meng. *J. Chem. Soc., Dalton Trans.*, 282 (2003).

[8] (a) G. Li, H.W. Hou, L.K. Li, X.R. Meng, Y.T. Fan, Y. Zhu. *Inorg. Chem.*, **42**, 4995 (2003); (b) G. Li, H.W. Hou, Z.F. Li, X.R. Meng, Y.T. Fan. *New J. Chem.*, **28**, 1595 (2004); (c) H.W. Hou, L.K. Li, Y. Zhu, Y.T. Fan, Y.Q. Qiao. *Inorg. Chem.*, **43**, 4767 (2004); (d) L.K. Li, Y.L. Song, H.W. Hou, Y.T. Fan, Y. Zhu. *Eur. J. Inorg. Chem.*, 3238 (2005); (e) L.K. Li, J.P. Li, H.W. Hou, Y.T. Fan, Y. Zhu. *Inorg. Chim. Acta*, **359**, 3139 (2006).

[9] X. Li, W. Liu, H.Y. Zhang, B.L. Wu. *J. Organomet. Chem.*, **693**, 3295 (2008).

[10] G.M. Sheldrick. *SHELXL93*, University of Göttingen, Germany (1993).

[11] Y. Qi, Y.X. Che, F. Luo, S.R. Batten, Y. Liu, J.M. Zheng. *Cryst. Growth Des.*, **8**, 1654 (2008).

[12] F.A. Cotton, L.R. Fallvello, A.H. Reid, J.H. Tocher. *J. Organomet. Chem.*, **319**, 87 (1987).

[13] D. Armentano, G. de Munno, F. Guerra, J. Faus, F. Lloret, M. Julve. *Dalton Trans.*, 4626 (2003).